



OPEN ACCESS

EDITED BY

Rita Pavasini,
University Hospital of Ferrara, Italy

REVIEWED BY

Ionut Donoiu,
University of Medicine and Pharmacy of
Craiova, Romania
Sergej Yelenski,
University Hospital RWTH Aachen,
Germany

*CORRESPONDENCE

Yang Zhang
✉ drzhy001@163.com

RECEIVED 20 November 2025

REVISED 05 March 2026

ACCEPTED 05 March 2026

PUBLISHED 27 March 2026

CITATION

Ren R, Zhao Q, Li W, Zhang Y, Xu X, Lv L
and Zhang Y (2026) Prognostic value of
mitral annular plane systolic excursion
for adverse cardiovascular events in
patients with acute myocarditis.
Front. Cardiovasc. Med. 13:1733925.
doi: 10.3389/fcvm.2026.1733925

COPYRIGHT

© 2026 Ren, Zhao, Li, Zhang, Xu, Lv and
Zhang. This is an open-access article
distributed under the terms of the
[Creative Commons Attribution License
\(CC BY\)](#). The use, distribution or
reproduction in other forums is
permitted, provided the original author(s)
and the copyright owner(s) are credited
and that the original publication in this
journal is cited, in accordance with
accepted academic practice. No use,
distribution or reproduction is permitted
which does not comply with these
terms.

Prognostic value of mitral annular plane systolic excursion for adverse cardiovascular events in patients with acute myocarditis

Ruichen Ren^{1,2}, Qingyuan Zhao¹, Wenting Li¹, Ying Zhang^{1,3},
Xinghua Xu¹, Lei Lv¹ and Yang Zhang^{1*}

¹Department of Radiology, Qilu Hospital of Shandong University, Jinan, China, ²Department of
Radiology, Beijing YouAn Hospital, Capital Medical University, Beijing, China, ³Department of
Ultrasound, Xiaojin County People's Hospital, Dezhou, China

Purpose: Mitral annular plane systolic excursion (MAPSE) has prognostic value as
a surrogate indicator of ventricular function in cardiovascular disease, but its
prognostic value in patients with acute myocarditis is unclear.

Methods: Our cohort included 46 patients with acute myocarditis and 26
healthy controls, all of whom underwent cardiac magnetic resonance. Left
atrial and left ventricular strain and MAPSE were assessed using feature
tracking, and patients were followed up in a group that experienced a major
adverse cardiovascular event (MACE) ($n = 11$) and a group that did not
experience a MACE ($n = 35$). Cox regression modelling was used to assess the
prognostic value of MAPSE in acute myocarditis.

Results: Left ventricular strain parameters (including global longitudinal,
circumferential, and radial strain), left atrial strain parameters (reservoir and
conduit strain), and MAPSE were significantly reduced compared with patients
without MACE. Receiver operating characteristic (ROC) curve showed that
MAPSE had a higher area under the curve (AUC) in identifying MACE. By
Kaplan–Meier analysis, the risk of death increased significantly with decreasing
lateral and septal MAPSE (log-rank $P = 0.0025$, $P = 0.0065$). After adjusting for
clinical and imaging risk factors, age (HR 1.139, 95%CI 1.056–1.228), lateral
MAPSE (HR 0.594, 95%CI 0.355–0.955), and septal MAPSE (HR 0.647, 95%CI
0.420–0.995) were significantly associated with MACE. The ROC curves
showed that the model including both lateral and septal MAPSE did not
improve predictive performance compared to lateral MAPSE alone
(AUC = 0.8831 vs. AUC = 0.9095).

Conclusion: MAPSE has prognostic value for adverse cardiovascular events in
patients with acute myocarditis, and lateral MAPSE has better predictive
performance.

KEYWORDS

cardiac magnetic resonance imaging, feature tracking, mitral annular plane systolic
excursion, myocarditis, prognostic

1 Introduction

Myocarditis is an acute or chronic inflammatory disease of the myocardium that can be caused by infection, immune response, or toxic injury (1). Symptoms of myocarditis vary from subclinical disease to chest pain with acute coronary syndrome-like manifestations, refractory cardiogenic shock, or sudden cardiac death due to ventricular fibrillation (2, 3). Myocarditis is the leading cause of sudden cardiac death and dilated cardiomyopathy (4, 5).

Cardiac magnetic resonance imaging has become the primary non-invasive method for diagnosing myocarditis and risk stratification (6). Conventional left ventricular ejection fraction (LVEF) is not sensitive enough to assess myocardial systolic function, and it is difficult to identify subtle but important changes in left ventricular (LV) systolic function (7). Cardiac magnetic resonance (CMR) feature tracking can be used to quantify biventricular and atrial deformations, displacements, torsions, and dyssynchrony (8). Several studies have shown that LV and left atrial (LA) strain is impaired in patients with acute myocarditis and can be a predictor of adverse prognosis (9, 10).

Atrial plane motion is an easy-to-measure surrogate for ventricular function, and reduced valve plane motion on echocardiography has been shown to be a predictor of adverse events in patients with a variety of cardiovascular diseases (11, 12). Impaired MAPSE on CMR is an independent determinant of all-cause mortality in patients with reduced LVEF (<50%) and predicts major adverse cardiovascular events in mixed populations, including patients with coronary artery disease or previous myocardial infarction, for major adverse cardiovascular events (13, 14). However, impaired MAPSE in patients with acute myocarditis has not been evaluated to date for its impairment and prognostic significance. Therefore, this study aimed to investigate the correlation of CMR-derived MAPSE with indices of atrial ventricular strain and to assess its predictive value for adverse cardiovascular events in patients with acute myocarditis.

2 Methods

This retrospective study was approved by our institutional ethics committee and written informed consent was waived; patient details were not disclosed.

2.1 Study population

We retrospectively analysed the medical records of 59 patients diagnosed with clinically suspected myocarditis and who underwent CMR from January 2016 to July 2024. The clinical diagnosis of suspected myocarditis was in accordance with the 2013 European Society of Cardiology guidelines (5). Diagnostic criteria included elevated troponin, ECG abnormalities, and structural or functional abnormalities confirmed by echocardiography or CMR. Patients with cardiac symptoms (chest pain, dyspnea or palpitations) who fulfilled one or more of the diagnostic criteria, as well as patients who

did not have any symptoms but fulfilled two or more of the above criteria, were identified as clinically suspected of having myocarditis. Exclusion criteria included coronary artery disease, non-ischemic cardiomyopathy, heart valve disease, Kawasaki disease and congenital heart disease. A total of 48 patients were included.

Baseline characteristics of patients at the time of CMR examination were collected, including demographic characteristics (age, sex, and body mass index [BMI]), cardiovascular risk factors (hypertension, diabetes mellitus), and laboratory findings (N-terminal pro-B-type natriuretic peptide (NT-proBNP), high-sensitivity cardiac troponin I [hs-TNI], white blood cell counts, and creatine kinase (CK)).

All patients were followed up by a radiologist (R.R.C., with 2 years of CMR experience) by chart review or telephone interview. The primary endpoint was major adverse cardiovascular events, defined as cardiac death, cardiogenic shock, new-onset heart failure, and readmission for recurrence of myocarditis or exacerbation of heart failure. Two patients (4.07%) were lost to follow-up and were not included in further outcome analyses. 46 patients were finally included.

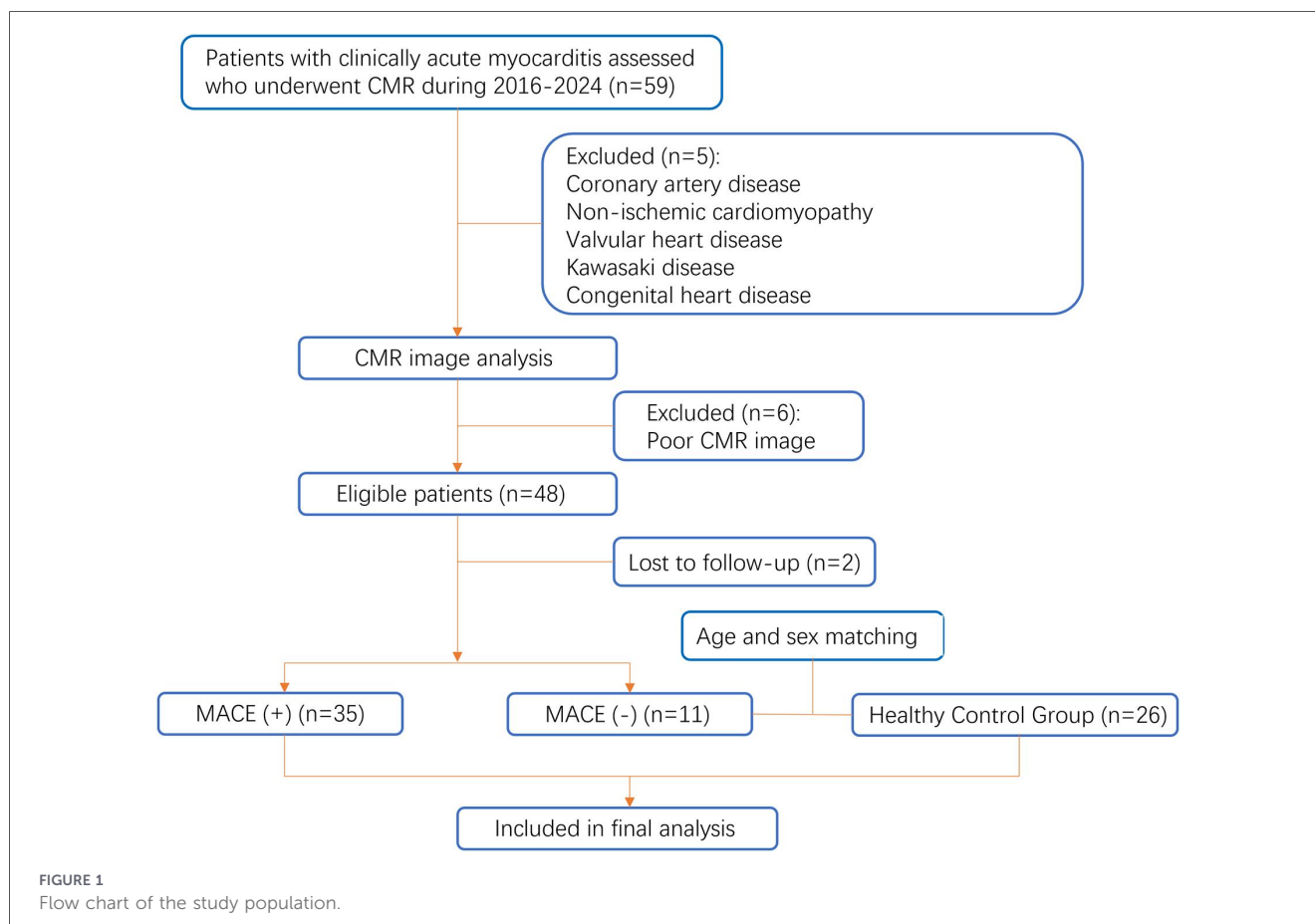
Twenty-six healthy volunteers who were age and gender matched, had no history of cardiovascular disease, normal ECG results, and no abnormal manifestations on CMR examination were selected as the healthy control group. The flow chart of the study is shown in Figure 1.

2.2 CMR protocols

CMR acquisition was performed using a SIEMENS MAGNETOM 1.5 T scanner (SIEMENS Healthcare, USA) equipped with an 8-channel phased array cardiac coil. The patient was in the supine position during acquisition. The CMR scanning protocol included cine imaging and late gadolinium enhancement (LGE) imaging. True Fast Imaging with Steady-state Precession (TrueFISP) end-expiratory breath-hold cine images were acquired to obtain 25 long-axis two- and four-chamber views and 9–11 short-axis slices covering the entire left ventricle from the mitral annulus to the apical epicardium. Typical cine imaging parameters were as follows: repetition time (TR)/echo time (TE), 48 ms/1.5 ms; flip angle (FA), 55°; matrix, 170 × 208; field of view (FOV), 256 × 209 mm; and slice thickness, 8 mm. 10–15 min after intravenous bolus injection of 0.2 mmol/kg Gd-DTPA (Bayer Magnevist, Berlin, Germany), myocardial LGE images were acquired using a Phase Sensitive Inversion Recovery (PSIR). Long-axis and short-axis view images were acquired at the same locations as the cine images. The parameters of the LGE sequence were as follows: TR/TE/FA, 804 ms/1.4 ms/45°; matrix, 143 × 256; FOV, 350 × 273 mm; slice thickness, 8 mm.

2.3 CMR image post processing

Image post-processing was performed by a radiologist (R.C.R.) with 2 years of experience in interpreting CMR images using commercial Cvi42 software (version 6.1.2, Circle, Calgary, Canada). A cohort of 19 patients was randomly selected to



assess interobserver agreement (with another radiologist (WT.L. with 2 years of CMR experience) prior to feature tracking analysis. The first radiologist also repeated the analysis after a 2-week interval to assess intraobserver agreement. Each radiologist (the two radiologists mentioned, RC.R., WT.L.) reviewed all LGE images for the presence or absence of nonischemic myocardial injury. When there was any difference opinion, agreement was reached after discussion with among three another radiologists (RC.R., WT.L. and Y.Z.) with 20 years of experience).

2.4 LA, LV volume and function analysis

End-systole and end-diastole of the LV in short-axis cine images were automatically defined, as well as the endocardium and epicardium of the LV in each section from the apical to the mitral valve plane. Papillary muscles were included in the LV volume. The LV volume and functional parameters were calculated and normalized to body surface area (BSA): LV end-diastolic volume index (LVEDVI), LV end-systolic volume index (LVESVI), LV stroke volume index (LVSVI), and LV mass index (LVMI).

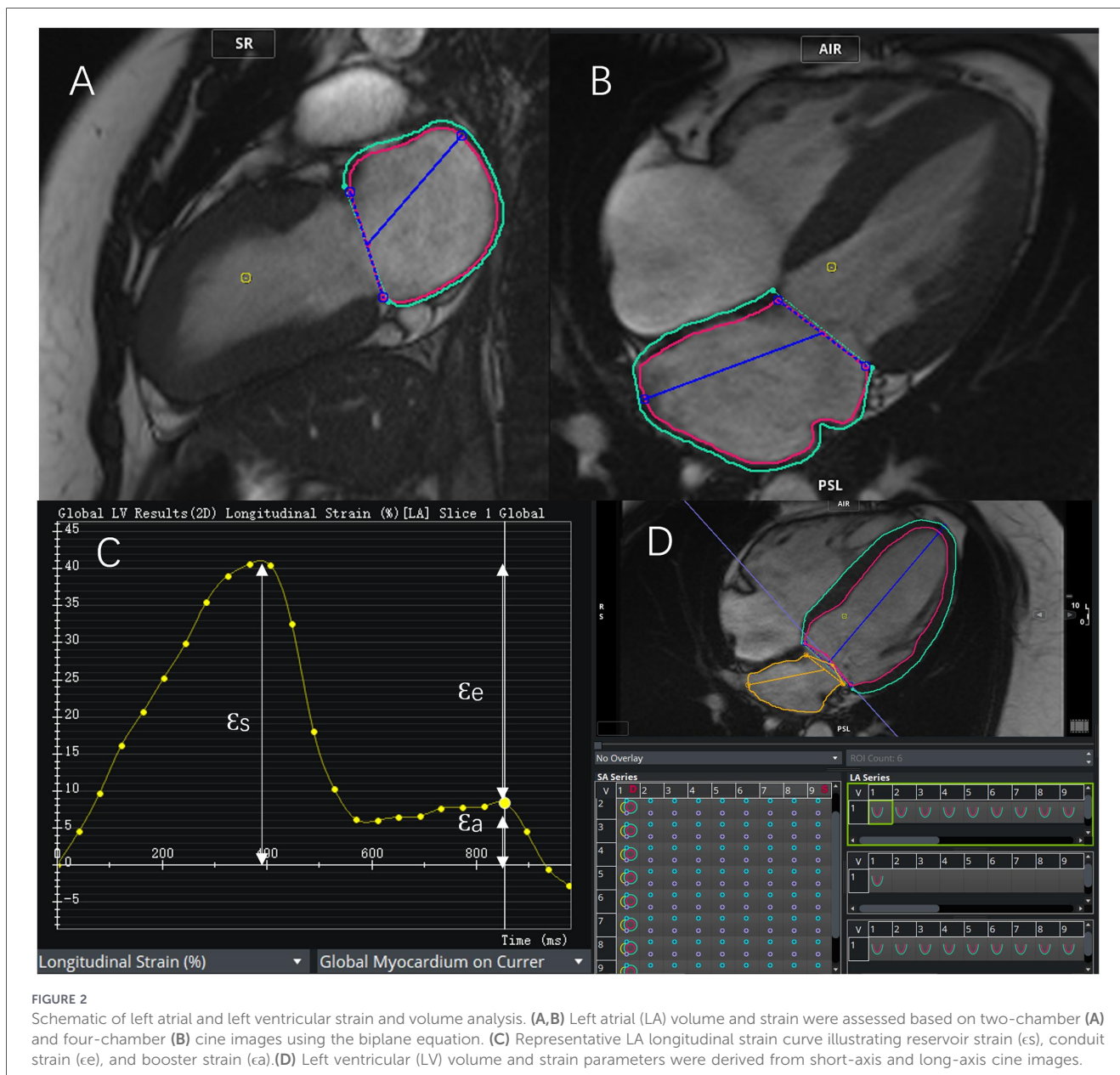
The end-diastolic phase of all cine images (including short-axis and 2-chamber, 3-chamber, and 4-chamber views) was selected for overall LV strain analysis. The software automatically calculated LV global radial strain (LVGRS), LV

global circumferential strain (LVGCS), and LV global longitudinal strain (LVGLS).

LA volume and function analysis were performed using cine images in 2-chamber and 4-chamber views. The inner edge of the LA (excluding LA appendages and pulmonary veins) was defined in three phases: LV end-systole (LAVmax) and end-diastole before (LAVpre) and after (LAVmin) LA contraction. These were normalized based on BSA to obtain the LAVmax index and the LAVpre index. LA functional parameters, including total LAEF, passive LAEF, and active LAEF. Also in the 2-chamber and 4-chamber views of the cine images, the left atrial border was manually depicted at the end of LV systole. LV strain metrics, including reservoir strain (ϵ_s), conduit strain (ϵ_c), and booster strain (ϵ_a), were automatically derived from the longitudinal strain curves. The LACI was calculated as the ratio of LAVmin to LVEDV and expressed as a percentage. The above analysis is shown in [Figure 2](#).

2.5 MAPSE measurement

The end-diastolic and end-systolic mitral annular planes were defined in cine images of the 4-chamber view, MAPSE was automatically measured. The mitral annular tracking points were adjusted on an image-by-image basis. Lateral MAPSE was defined as the distance from end-systole to end-diastole at the lateral attachment point in the mitral valve. Septal MAPSE was



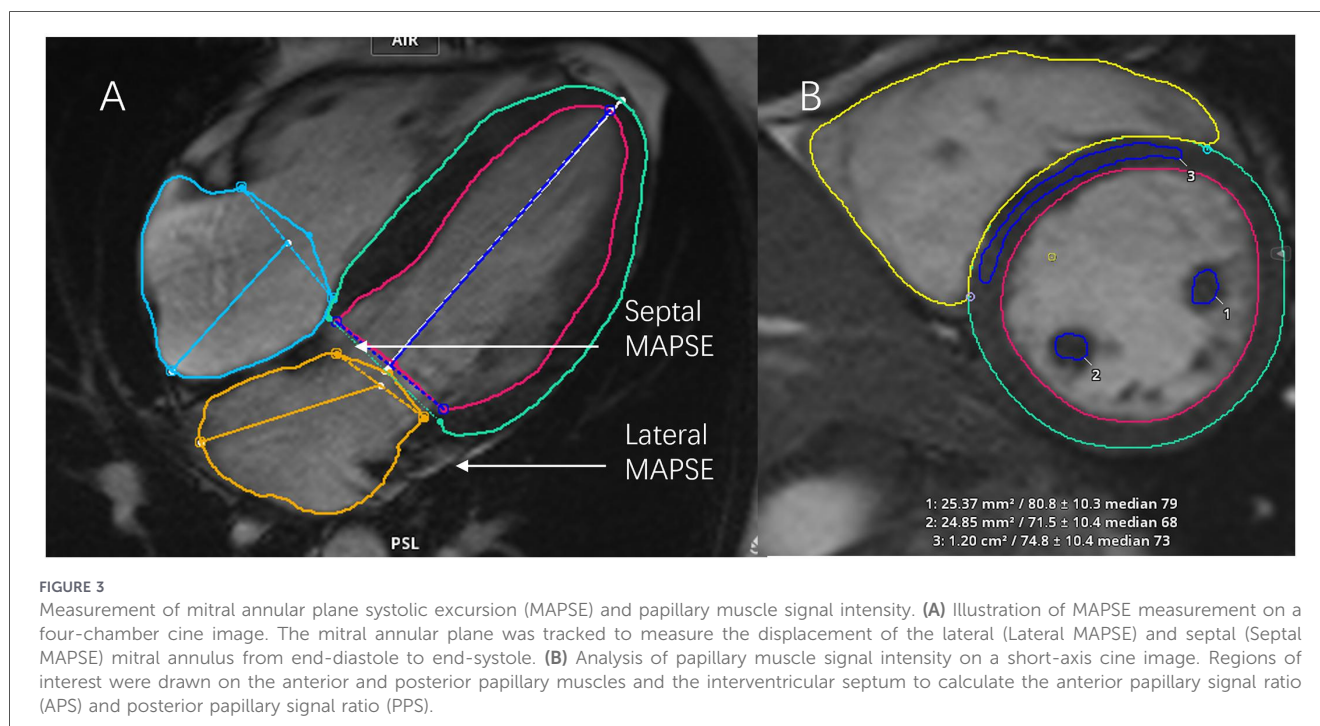
defined as the distance from end-systole to end-diastole at the attachment point of the mitral valve in the septum. The above analysis is shown in Figure 3.

2.6 Signal ratio of the papillary muscle measurement

The papillary muscle signals were measured at end-systole by selecting the short-axis cine view. The regions of interest of the left ventricular anterior papillary muscle, posterior papillary muscle, and interventricular septum were manually plotted separately. The inclusion of the left ventricular cavity signal was avoided as much as possible. Finally, the anterior papillary muscle signal, posterior papillary muscle signal, and left ventricular septum signal were compared to obtain the anterior papillary signal ratio (APS) and posterior papillary signal ratio (PPS), respectively. The above analysis is shown in Figure 3.

2.7 Statistical analysis

All data were analysed using SPSS Statistics (Version-26.0; IBM Corp) and GraphPad Prism (Version-10.2; GraphPad Software Inc.). Continuous variables are expressed as mean \pm standard deviation, and for normal distributions, comparisons were made using independent samples *t*-tests. For non-normal distributions, expressed as the median and interquartile range (IQR), comparisons were made using the Mann–Whitney *U* test. Categorical variables were expressed as counts and percentages and were compared using chi-square or Fisher's exact tests as needed. The occurrence of adverse clinical endpoints in the high- and low-risk groups was assessed using Kaplan–Meier survival analyses after setting MACE high/low risk cut-offs using ROC curve analysis. Graphs were compared using the log-rank test. Associations of CMR parameters with MACE were determined using univariate and multivariate Cox proportional risk regression analyses. The proportional hazards



assumption was verified using Schoenfeld residuals, and the assumption was met for all included variables. Parameters with P values <0.05 in univariate analyses were included in multivariate analyses. Results are reported as risk ratios (HR) and 95% confidence intervals (CI). Correlations between LV strain, LA strain, LACI, and MAPSE were determined using linear regression. Reproducibility analyses were performed using intragroup correlation coefficients (ICC) to determine inter- and intra-observer agreement. P -values <0.05 were considered statistically significant.

3 Results

3.1 Study population

This study retrospectively analyzed 46 patients with acute myocarditis and 26 age- and sex-matched healthy people as controls. After a median follow-up period of 740 (IQR: 513.4–966.6) days, 11 patients (23.91%) with MACE, including cardiac death (3 patients, 6.52%), cardiogenic shock (4 patients, 8.70%), and rehospitalization due to recurrence of myocarditis or exacerbation of heart failure (4 patients, 8.70%).

3.2 Clinical characteristics and baseline data of patients with and without MACE and normal controls

Baseline characteristics are summarized in Table 1. Heart rate was higher in patients with MACE, with no significant difference between the two comparisons. In addition, hs-TNI levels were higher in patients without MACE (0.92 ng/mL [IQR: 0.04–3.39 ng/mL] vs. 0.02 ng/mL [IQR: 0.01–0.96 ng/mL]).

3.3 Cardiac magnetic resonance-derived LA, LV volume and functional parameters and mitral annular displacement and papillary muscle signal intensity analysis

CMR parameters are shown in Table 2. LVSVI and LVEF were significantly lower in patients with MACE than in normal controls (29.07 ± 11.34 mL/m² vs. 38.64 ± 8.32 mL/m² and 37.47% [IQR: 20.74–56.98%] vs. 57.10% [IQR: 54.17–60.18%], respectively). LV strain parameters (LVGLS, LVGCS, LVGRS) were significantly lower in patients with MACE than in normal controls vs. patients who did not develop MACE ($-9.16 \pm 3.03\%$ vs. $-16.8 \pm 3.55\%$ vs. $-15.85 \pm 6.69\%$, respectively, and -8.7% [IQR: -14.3 – -6.6%] vs. -19.0% [IQR: -20.4 – -16.5%] vs. -17.8% [IQR: -19.2 – -12.8%], 13.8% [IQR: 8.3–21.7%] vs. 32.2% [IQR: 25.8–36.0%] vs. 29.9% [IQR: 19.1–33.7%]). In contrast, LV strain parameters in patients without MACE were not significantly different from normal controls.

For LA volume and functional parameters, total LAEF was significantly lower in patients with MACE ($57.40 \pm 12.99\%$ vs. $52.52 \pm 15.53\%$ vs. $66.64 \pm 7.18\%$) and passive LAEF was significantly lower in patients with MACE ($34.24 \pm 9.48\%$ vs. $39.75 \pm 7.41\%$), whereas booster LAEF was significantly lower in patients without MACE ($35.97 \pm 12.96\%$ vs. $44.62 \pm 10.18\%$).

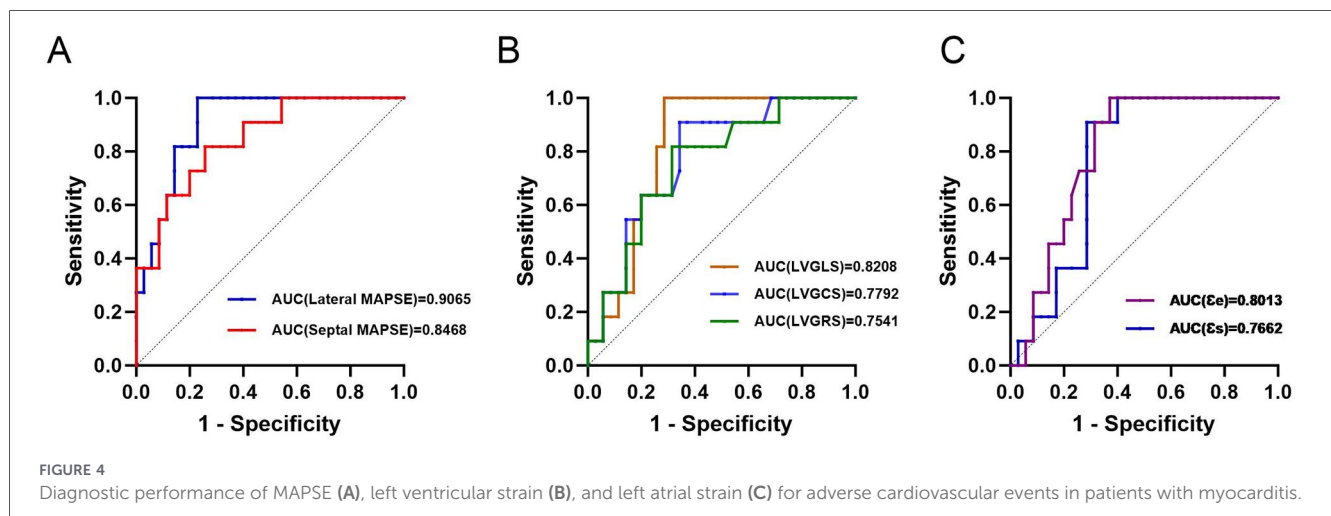
For LA strain parameters, cs and ce were significantly lower in patients without MACE and in patients with MACE compared with normal controls (28.3% [IQR: 16.7–36.3%] vs. 18.2% [IQR: 15.2–20.6%] vs. 34.5% [IQR: 28.8–47.8%], 15.3% [IQR: 10.3–24.1%] vs. 8.6% [IQR: 5.8–12.0%] vs. 23.0% [IQR: 18.6–32.3%]). For both groups of patients with acute myocarditis, cs and ce were significantly impaired in patients.

For mitral annular displacement, septal MAPSE and lateral MAPSE were significantly lower in patients with MACE compared with the other two groups (14.51 ± 4.04 mm vs.

TABLE 1 Baseline characteristics.

Characteristics	All Patients (N = 46)		Control group (N = 26)	P value
	MACE(-) (N = 35)	MACE(+) (N = 11)		
Demographic characteristics				
Age, years	28 (17, 39)	32 (20, 61)	26 (18, 40)	0.600
Sex, male, N (%)	25 (71.4)	6 (54.5)	15 (57.7)	0.430
Body mass index, kg/m ²	23.54 ± 4.56	24.07 ± 5.11	24.88 ± 3.83	0.502
Heart rate, beat/min	66 (58, 102)	80 (70, 91)	74 (69, 81)	0.015
Cardiovascular risk factors				
Hypertension, N (%)	4 (11.4)	3 (27.3)	-	0.333
Diabetes mellitus, N (%)	2 (5.7)	2 (18.2)	-	0.238
Laboratory results				
NT-proBNP, pg/mL	1,151 (141, 1,747)	826 (173, 3,363)	-	0.780
hs-TNI, ng/mL	0.92 (0.04, 3.39)	0.02 (0.01, 0.96)	-	0.018
WBC count, × 10 ⁹ /L	8.47 (6.92, 12.03)	9.07 (6.3, 13.66)	-	0.975
CK, U/L	97 (51, 161)	93 (65, 191)	-	0.844

MACE, major adverse cardiac events; NT-proBNP, N-terminal pro-B-type natriuretic peptide; hs-TNI, high-sensitivity cardiac troponin I; WBC, white blood cells; CK, creatine kinase. For variables available in all three groups (Age, Sex, BMI, Heart rate), *P*-values represent the comparison among the three groups (MACE+, MACE-, and Control) using One-way ANOVA, Kruskal-Wallis test, or Chi-square test. For variables unavailable in the Control group (Hypertension, Diabetes mellitus, and laboratory results), *P*-values represent the comparison between MACE(+) and MACE(-) groups using Mann-Whitney *U* test or Fisher's exact test.



9.24 ± 3.20 mm vs. 17.33 ± 3.06 mm, 9.97 mm [IQR: 8.88–11.01 mm] vs. 6.98 mm [IQR: 3.91–8.55 mm] vs. 13.53 mm [IQR: 11.44–14.9 mm]).

There was no significant difference in the signal ratio of the papillary muscles between the three groups.

3.4 Diagnostic performance of myocardial strain parameters and MAPSE for MACE in patients with myocarditis

We evaluated the diagnostic performance of myocardial strain parameters and MAPSE in identifying adverse cardiovascular events in patients with myocarditis using ROC curve analysis. Results

showed (Figure 4) good diagnostic performance of left ventricular strain, left atrial reservoir and conduit strain, and MAPSE. The AUC was higher for septal MAPSE and lateral MAPSE.

We determined the optimal lateral MAPSE of 11.96 mm and the optimal septal MAPSE cutoff value (Youden index) of 8.85 mm, respectively, in the entire cohort to better categorize the patients into low-risk and high-risk groups (Figure 5).

Table 3 shows the results of univariate and multivariate Cox regression analyses. In univariate analysis, age, ϵ_e , septal MAPSE, and lateral MAPSE were significantly associated with MACE occurrence (HR 1.044, 95% CI 1.006–1.084; HR 0.872, 95% CI 0.761–1.000; HR 0.755, 95% CI 0.627–0.909; HR 0.707, 95% CI 0.568–0.880). These were selected for multifactorial analysis, which showed that age, septal MAPSE and lateral

TABLE 2 CMR parameters.

Parameters	All Patients (N = 46)		Control group (N = 26)	P value
	MACE(-) (N = 35)	MACE(+) (N = 11)		
LV parameters				
LVEDVI, mL/m ²	63.11 (55.65, 87.6)	72.63 (65.11, 108.00)	69.84 (58.3, 79.31)	0.534
LVESVI, mL/m ²	28.43 (24.64, 41.84)	52.77 (29.41, 67.52)	30.35 (23.79, 34.32)	0.156
LVSVI, mL/m ²	33.48 ± 10.61	29.07 ± 11.34	38.64 ± 8.32 ^b	0.022
LVEF, %	53.19 (46.93, 59.39)	37.47 (20.74, 56.98)	57.10 (54.17, 60.18) ^b	0.008
LVMI, g/m ²	44.40 (40.39, 58.40)	43.24 (39.97, 56.14)	43.63 (35.88, 50.60)	0.321
LVGLS, %	-15.85 ± 6.69	-9.16 ± 3.03 ^a	-16.8 ± 3.55 ^b	0.001
LVGCS, %	-17.8 (-19.2, -12.8)	-8.7 (-14.3, -6.6) ^a	-19.0 (-20.4, -16.5) ^b	0.001
LVGRS, %	29.9 (19.1, 33.7)	13.8 (8.3, 21.7) ^a	32.2 (25.8, 36.0) ^b	0.002
Presence of LGE	19 (0.54)	5 (0.45)	-	0.734
LA parameters				
LAVImax, mL/m ²	30.44 ± 9.99	28.72 ± 11.57	29.28 ± 8.09	0.830
LAVImin, mL/m ²	12.24 (8.21, 16.75)	9.20 (7.75, 21.8)	9.64 (6.74, 12.53)	0.160
LAVIpre, mL/m ²	19.75 (13.88, 25.82)	17.23 (12.12, 26.55)	17.17 (12.75, 23.34)	0.500
Total LAEF, %	57.40 ± 12.99	52.52 ± 15.53	66.64 ± 7.18 ^{a,b}	0.001
Passive LAEF, %	34.24 ± 9.48	28.39 ± 14.54	39.75 ± 7.41 ^b	0.005
Booster LAEF, %	35.97 ± 12.96	33.84 ± 16.03	44.62 ± 10.18 ^a	0.014
es, %	28.3 (16.7, 36.3)	18.2 (15.2, 20.6) ^a	34.5 (28.8, 47.8) ^{a,b}	0.001
ee, %	15.3 (10.3, 24.1)	8.6 (5.8, 12.0) ^a	23.0 (18.6, 32.3) ^{a,b}	0.001
ea, %	12.1 (8.1, 13.6)	7.8 (6.2, 9.8)	11.8 (9.7, 13.6)	0.112
LACI, %	18.18 ± 7.27	16.64 ± 6.40	14.95 ± 5.87	0.181
MAPSE				
Septal MAPSE, mm	14.51 ± 4.04	9.24 ± 3.20 ^a	17.33 ± 3.06 ^{a,b}	0.001
Lateral MAPSE, mm	9.97 (8.88, 11.01)	6.98 (3.91, 8.55) ^a	13.53 (11.44, 14.9) ^{a,b}	0.001
Papillary muscle signal ratio				
APS	1.05 (0.90, 1.14)	1.04 (0.97, 1.10)	1.06 (0.99, 1.12)	0.615
PPS	1.06 (0.91, 1.19)	1.12 (0.96, 1.21)	1.04 (0.93, 1.17)	0.673

LV, left ventricular; LVEDVI, left ventricular end diastolic volume index; LVESVI, left ventricular end systolic volume index; LVSVI, left ventricular stroke volume index; LVEF, left ventricular ejection fraction; LVMI, LV mass index; LVGLS, left ventricular global longitudinal strain; LVGCS, left ventricular global circumferential strain; LVGRS, left ventricular global radial strain; LA, left atrial; LAVImax, maximum left atrial volume index; LAVImin, minimum left atrial volume index; LAVIpre, left atrial volume index at end-diastole before LA contraction; LAEF, left atrium ejection fraction; es, reservoir strain; ee, conduit strain; ea, booster strain; LACI, left atrioventricular coupling index; MAPSE, mitral annular plane systolic excursion; APS, anterior papillary signal ratio; PPS, posterior papillary signal ratio.

^aCompared with MACE(+).

^bCompared with MACE(+).

MAPSE were independent predictors of MACE (HR 1.141, 95% CI 1.058–1.231; HR 0.673, 95% CI 0.453–0.998; HR 0.544, 95% CI 0.333–0.890; respectively).

We combined variables with independent predictive value from multifactor Cox regression analysis into different Cox regression models. The results (Figure 6) showed that the model with both lateral and septal MAPSE did not improve predictive performance compared with lateral MAPSE alone (AUC = 0.8831 vs. AUC = 0.9095). Figure 6 showed that the model with the addition of age had a higher predictive value (AUC = 0.8701 vs. AUC = 0.8468, AUC = 0.9221 vs. AUC = 0.9065, and AUC = 0.9091 vs. AUC = 0.8831), but similarly, the addition of interventricular MAPSE did not improve predictive performance

with the addition of age plus lateral MAPSE compared to interventricular MAPSE (AUC = 0.9091 vs. AUC = 0.9221).

3.5 Correlation between MAPSE and other CMR parameters in patients and control group

MAPSE was moderately correlated with LA and LV strain parameters. Septal MAPSE and LACI were poorly correlated. Lateral MAPSE did not correlate significantly with LACI. MAPSE did not correlate significantly with any of the papillary muscle signal ratios. The details of correlations were presented in Table 4.

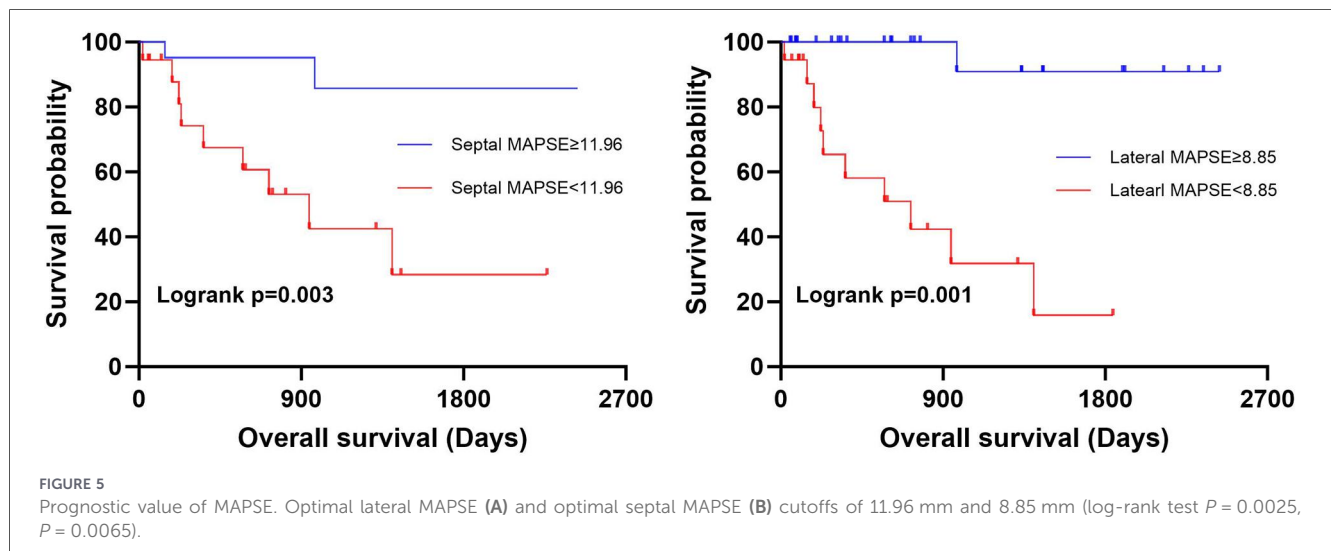


TABLE 3 Univariate and multivariate Cox regression analyses used to predict MACE.

Variables	Univariable analysis		Multivariable analysis	
	Hazard ratio (95% CI)	<i>P</i> value	Hazard ratio (95% CI)	<i>P</i> value
Age, years	1.044 (1.006, 1.084)	0.022	1.139 (1.056, 1.228)	0.001
Heart rate, beat/min	1.025 (0.996, 1.055)	0.092		
LVEDVI, mL/m ²	1.005 (0.983, 1.027)	0.683		
LVESVI, mL/m ²	1.008 (0.991, 1.026)	0.358		
LVSVI, mL/m ²	0.959 (0.904, 1.018)	0.172		
LVEF, %	0.981 (0.947, 1.015)	0.267		
LVGLS, %	1.140 (1.015, 1.281)	0.027	0.867 (0.660, 1.139)	0.306
LVGCS, %	1.123 (0.999, 1.261)	0.051		
LVGRS, %	0.947 (0.893, 1.003)	0.064		
Presence of LGE	1.722 (0.523, 5.681)	0.373		
LAVImax, mL/m ²	0.973 (0.911, 1.039)	0.410		
LAVImin, mL/m ²	1.004 (0.940, 1.072)	0.900		
LAVIpre, mL/m ²	1.000 (0.935, 1.069)	0.995		
Total LAEF, %	0.986 (0.951, 1.021)	0.426		
Passive LAEF, %	0.955 (0.903, 1.008)	0.097		
Booster LAEF, %	0.995 (0.955, 1.036)	0.797		
cs, %	0.931 (0.859, 1.008)	0.079		
ce, %	0.872 (0.761, 1.000)	0.050	0.898 (0.706, 1.142)	0.381
ca, %	0.928 (0.799, 1.078)	0.327		
LACI, %	0.995 (0.913, 1.085)	0.909		
Septal MAPSE, mm	0.755 (0.627, 0.909)	0.003	0.647 (0.420, 0.995)	0.047
Lateral MAPSE, mm	0.707 (0.568, 0.880)	0.002	0.594 (0.355, 0.995)	0.048
APS	3.341 (0.079, 141.023)	0.528		
PPS	6.980 (0.256, 190.324)	0.249		

LVEDVI, left ventricular end diastolic volume index; LVESVI, left ventricular end systolic volume index; LVSVI, left ventricular stroke volume index; LVEF, left ventricular ejection fraction; LVGLS, left ventricular global longitudinal strain; LVGCS, left ventricular global circumferential strain; LVGRS, left ventricular global radial strain; LAVImax, maximum left atrial volume index; LAVImin, minimum left atrial volume index; LAVIpre, left atrial volume index at end-diastole before LA contraction; LAEF, left atrium ejection fraction; cs, reservoir strain; ce, conduit strain; ca, booster strain; LACI, left atrioventricular coupling index; MAPSE, mitral annular plane systolic excursion; APS, anterior papillary signal ratio; PPS, posterior papillary signal ratio.

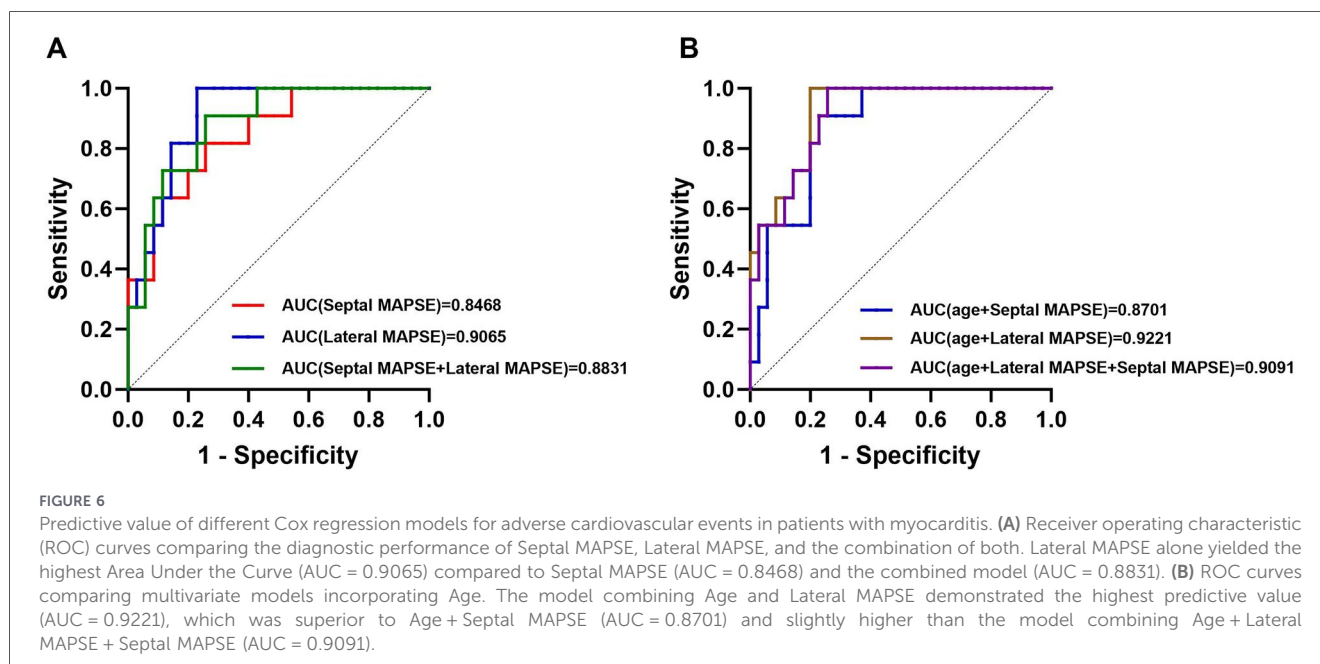


TABLE 4 Correlation between MRI parameters and MAPSE.

Parameters	Septal MAPSE		Lateral MAPSE	
	<i>r</i>	<i>P</i>	<i>r</i>	<i>P</i>
LVEF, %	0.335	0.004	0.493	0.001
LVGLS, %	-0.644	0.001	-0.595	0.001
LVGCS, %	-0.560	0.001	-0.537	0.001
LVGRS, %	0.519	0.001	0.482	0.001
LGE, n	0.051	0.737	-0.157	0.296
es, %	0.552	0.001	0.615	0.001
ce, %	0.547	0.001	0.597	0.001
ca, %	0.378	0.001	0.427	0.001
LACI, %	-0.253	0.032	-0.137	0.252
APS	0.108	0.368	0.030	0.801
PPS	0.029	0.809	-0.108	0.369

LVEF, left ventricular ejection fraction; LVGLS, left ventricular global longitudinal strain; LVGCS, left ventricular global circumferential strain; LVGRS, left ventricular global radial strain; es, reservoir strain; ce, conduit strain; ca, booster strain; LACI, left atrioventricular coupling index; MAPSE, mitral annular plane systolic excursion; APS, anterior papillary signal ratio; PPS, posterior papillary signal ratio.

3.6 Reproducibility analysis

As shown in Table 5, LA and LV strains and MAPSE showed excellent intraobserver and interobserver agreement.

4 Discussion

This study focused on the prognostic value of mitral annular plane systolic excursion in acute myocarditis and compared it with left atrial

and left ventricular strain. The main findings were as follows: (1) Compared with normal controls, septal MAPSE and lateral MAPSE were decreased in patients with acute myocarditis. Compared with patients without MACE, septal MAPSE and lateral MAPSE were impaired in patients with MACE. (2) Compared with LA and LV strains, septal MAPSE and lateral MAPSE had higher diagnostic performance. (3) Septal MAPSE and lateral MAPSE can be used as prognostic factors for major adverse cardiovascular events in patients with acute myocarditis, and the predictive value of lateral MAPSE is even higher. (4) Septal MAPSE and lateral MAPSE have a good correlation with LA and LV strain.

The ventricular myocardium consists of an obliquely traveling endocardium and epicardium and a circumferentially traveling intermediate myocardium (15). One of the main purposes of the shear deformation of the left ventricle during contraction is to amplify the 15% shortening of the cardiomyocytes into a 40% radial left ventricular wall thickening, which in turn leads to a change in the left ventricular ejection fraction of >60% in a normal heart (16). Thus, the long-axis function of the heart plays an important role in the ejection activity of the heart. This may also explain the excellent diagnostic performance of global longitudinal strain (GLS) and global circumferential strain (GCS) in myocarditis (17), as well as in patients with acute myocarditis with preserved ejection fraction (18, 19). Throughout the cardiac cycle, the mitral annulus is pulled toward the apex, and the left ventricular cavity volume decreases, which prompts ventricular ejection. At this time the base of the atrium moves downward and the volume of the atrium increases thereby drawing blood from the pulmonary veins into the atria. During atrial contraction, the mitral annulus is pulled off the apex by the contracting atrial myocardium, further contributing to atrial emptying and ventricular filling (20–22). Basically, MAPSE is the result of contraction of both subendocardial and subepicardial longitudinal fibers (23). It has been demonstrated that up to 60% of the per-passage output

TABLE 5 Intra- and inter-observer variability of MRI parameters.

Parameters	Intraobserver		Interobserver	
	ICC (95% CI)	P Value	ICC (95% CI)	P Value
LVGLS, %	0.958 (0.896, 0.984)	<0.001	0.928 (0.826, 0.972)	<0.001
LVGCS, %	0.981 (0.953, 0.993)	<0.001	0.959 (0.797, 0.987)	<0.001
LVGRS, %	0.992 (0.980, 0.997)	<0.001	0.989 (0.972, 0.996)	<0.001
es, %	0.975 (0.937, 0.990)	<0.001	0.984 (0.959, 0.994)	<0.001
ee, %	0.972 (0.922, 0.990)	<0.001	0.976 (0.940, 0.991)	<0.001
ea, %	0.830 (0.618, 0.931)	<0.001	0.913 (0.792, 0.965)	<0.001
Septal MAPSE, mm	0.981 (0.953, 0.993)	<0.001	0.985 (0.962, 0.994)	<0.001
Lateral MAPSE, mm	0.987 (0.966, 0.995)	<0.001	0.984 (0.960, 0.994)	<0.001

LVGLS, left ventricular global longitudinal strain; LVGCS, left ventricular global circumferential strain; LVGRS, left ventricular global radial strain; es, reservoir strain; ee, conduit strain; ea, booster strain; MAPSE, mitral annular plane systolic excursion.

can be explained by the movement of the longitudinal mitral annulus (24, 25). LVGLS has a strong correlation and MAPSE is significantly impaired in patients with acute myocarditis. In our study, although LVGLS was significantly associated with MACE in the univariate analysis, it lost its significance in the multivariate model, whereas MAPSE remained an independent predictor. Both parameters evaluate longitudinal myocardial function and are inherently collinear. The superiority of MAPSE in our multivariate model may be attributed to its methodological robustness. LVGLS, derived from CMR feature tracking, heavily relies on optimal image quality and accurate endocardial border definition, which can be compromised by severe myocardial edema and late gadolinium enhancement typical of acute myocarditis. Conversely, MAPSE is a simple, direct anatomical measurement of annular displacement that is highly reproducible and less susceptible to image artifacts, making it a more stable prognostic marker in this specific cohort.

Measurement of MAPSE in patients with acute or chronic myocardial infarction using different echocardiographic methods has shown that MAPSE predicts the occurrence of adverse events (26, 27). Ultrasound is more sensitive to noise, which can be affected by the different angles of manipulation and inexperience of the operator (28). In contrast, CMR is more accurate and reproducible and does not require additional sequences and specific Software. The displacement of the mitral annulus relative to the apex measured by CMR was found to correlate well with the overall longitudinal strain measured by echocardiography (29). The present study demonstrated good intraobserver and interobserver agreement for CMR-derived MAPSE.

The present study demonstrated that both lateral and septal MAPSE have independent predictive value for adverse events in acute myocarditis, with lateral MAPSE having a higher value and a greater risk ratio. Of note, the predictive value of lateral and septal MAPSE was diminished when both were included in the prediction model compared with lateral MAPSE alone. Rangarajan et al. demonstrated that lateral MAPSE, as a surrogate for LV long-axis function, was an independent predictor of major adverse cardiovascular events using a CMR

routine movie sequence (14). Although LVEF was lower in the MACE group, MAPSE represents longitudinal function, which is governed by subendocardial fibers that are often more susceptible to ischemia and inflammation than the circumferential fibers responsible for LVEF. Therefore, MAPSE may serve as a more sensitive, early marker of myocardial dysfunction even before significant drops in ejection fraction occur. A large multicenter study demonstrated that lateral MAPSE is a significant independent predictor of mortality in patients with LV dysfunction and reduced ejection fraction and can provide more valuable prognostic information than conventional imaging indices, including ejection fraction and late gadolinium enhancement of the LGE (13). Differently, Mayr et al. found that septal MAPSE, compared with lateral and mean MAPSE, had a higher ST-segment-elevation MACE predictive value in patients with ST-segment-elevation myocardial infarction predictive value of MACE (30). This may be because lateral MAPSE is mainly influenced by left ventricular long-axis function, whereas septal MAPSE is also influenced by right ventricular reciprocal function. There are fewer data on the prevalence and prognostic significance of right ventricular involvement in patients with acute myocarditis. Aquaro et al. recruited 27 (17.8%) of 151 patients with clinically suspected acute myocarditis with signs of right ventricular involvement, and multivariate Cox regression analysis showed that right ventricular involvement was an independent predictor of cardiac events (31). Bernhard et al. included 659 patients with suspected myocarditis, and 162 (25.5%) had right ventricular involvement, with 162 (25.9%) patients showing impaired RVEF and 144 (21.9%) patients with impaired RV GLS, and multivariate Cox regression showed that right ventricular GLS provided only limited value in suspected myocarditis (32). Based on the results of the present study, we recommend the use of lateral MAPSE independent of right ventricular involvement to predict the occurrence of adverse cardiovascular events in patients with acute myocarditis.

Both left ventricular and left atrial strains were significantly reduced in patients who developed MACE in this study compared with patients with acute myocarditis who did not

develop MACE, and the ROC curves showed good discriminatory performance for adverse events for both of these strain parameters, whereas multifactorial cox regression did not show an independent predictive value, which we speculate may be related to the small sample size.

It has been found that the papillary muscle to LV wall myocardial signal ratio is low in patients with mitral valve prolapse, which has not been observed in other conditions that may affect the mitral annulus (33). This “dark papillary muscle sign” is an independent predictor of poor prognosis in patients with ventricular arrhythmias and normal LVEF, and may be due to a transient perfusion defect of the muscle during peak ventricular contraction (34). We analyzed the papillary muscle signal ratio, and our results showed that there was no significant correlation between the papillary muscle signal ratio and MAPSE. The reason may be that myocarditis is a disease that primarily involves the myocardium, and the papillary muscles are rarely involved. High signal in the myocardium is less frequently observed on cine sequences, and even less frequently in the septum. Deux et al. performed scanning cine, enhancement cine, and delayed gadolinium enhancement scans in 18 patients with acute myocarditis and showed that areas of high signal were detected on the scanning cine sequences in 28% (5/18) of the patients (35). Therefore, a larger cohort should be conducted in the future to explore the value of papillary muscle signal ratio in the diagnosis and prognosis of myocarditis.

This study has several limitations. First, this was a retrospective study spanning from 2016 to 2024. Advanced parametric mapping sequences (T1 and T2 mapping) were not routinely available or performed for all patients, particularly in the earlier years. Thus, the diagnosis relied on the 2013 ESC criteria and standard Lake Louise Criteria rather than the updated 2018 criteria. However, LGE and cine imaging were available for all patients to ensure robust functional and structural analysis. Second, the sample size and the number of MACE events ($n = 11$) in this single-center study were limited. Although this raises the risk of overfitting in the multivariate Cox regression, acute myocarditis cohorts with long-term CMR follow-up are inherently small. To mitigate this, we strictly limited the number of covariates, an approach consistent with similar recent studies (e.g., Lee et al. (10)). Nonetheless, these multivariate results should be considered exploratory and require validation in larger, multi-center cohorts. Third, the prolonged enrollment period (2016–2024) introduces potential confounding effects, as the evolution of heart failure pharmacotherapy over this 8-year span may have influenced individual clinical outcomes.

5 Conclusion

CMR-derived mitral annular systolic displacement has prognostic value for adverse cardiovascular events in patients with acute myocarditis, and correlates well with the left atrium and left ventricle. It can be used as a surrogate index of left ventricular function to evaluate the prognosis of patients with acute myocarditis.

Data availability statement

The raw data supporting the conclusions of this article will be made available by the authors, without undue reservation.

Ethics statement

The studies involving humans were approved by the Ethics Committee of the Qilu Hospital of Shandong University (Ethical Approval No. KYLL-202408-051-1). The studies were conducted in accordance with the local legislation and institutional requirements. The Ethics Committee/institutional review board waived the requirement of written informed consent for participation from the participants or the participants' legal guardians/next of kin because it is a retrospective study of clinical data without naming or privacy.

Author contributions

RR: Conceptualization, Writing – review & editing, Methodology, Writing – original draft, Formal analysis. QZ: Methodology, Writing – review & editing, Formal analysis, Validation. WL: Writing – review & editing, Formal analysis, Project administration. YZ: Supervision, Validation, Writing – review & editing. XX: Validation, Supervision, Writing – review & editing. LL: Writing – review & editing, Validation, Supervision. YZ: Funding acquisition, Methodology, Conceptualization, Writing – review & editing.

Funding

The author(s) declared that financial support was received for this work and/or its publication. This study has received funding by the Natural Science Foundation of Shandong Province (ZR2024ZD23).

Conflict of interest

The author(s) declared that this work was conducted in the absence of any commercial or financial relationships that could be construed as a potential conflict of interest.

Generative AI statement

The author(s) declared that generative AI was not used in the creation of this manuscript.

Any alternative text (alt text) provided alongside figures in this article has been generated by Frontiers with the support of artificial intelligence and reasonable efforts have been made to ensure accuracy, including review by the authors wherever possible. If you identify any issues, please contact us.

Publisher's note

All claims expressed in this article are solely those of the authors and do not necessarily represent those of their affiliated

organizations, or those of the publisher, the editors and the reviewers. Any product that may be evaluated in this article, or claim that may be made by its manufacturer, is not guaranteed or endorsed by the publisher.

References

- Sagar S, Liu PP, Cooper LT Jr. Myocarditis. *Lancet*. (2012) 379(9817):738–47. doi: 10.1016/s0140-6736(11)60648-x
- Mason JW, O'Connell JB, Herskowitz A, Rose NR, McManus BM, Billingham ME, et al. A clinical trial of immunosuppressive therapy for myocarditis. The myocarditis treatment trial investigators. *N Engl J Med*. (1995) 333(5):269–75. doi: 10.1056/nejm199508033330501
- Leone O, Pieroni M, Rapezzi C, Olivetto I. The Spectrum of myocarditis: from pathology to the clinics. *Virchows Arch*. (2019) 475(3):279–301. doi: 10.1007/s00428-019-02615-8
- Pollack A, Kontorovich AR, Fuster V, Dec GW. Viral myocarditis—diagnosis, treatment options, and current controversies. *Nat Rev Cardiol*. (2015) 12(11):670–80. doi: 10.1038/nrcardio.2015.108
- Caforio ALP, Pankuweit S, Arbustini E, Basso C, Gimeno-Blanes J, Felix SB, et al. Current state of knowledge on aetiology, diagnosis, management, and therapy of myocarditis: a position statement of the European Society of Cardiology working group on myocardial and pericardial diseases. *Eur Heart J*. (2013) 34(33):2636–48. doi: 10.1093/eurheartj/eh210
- Eichhorn C, Greulich S, Bucciarelli-Ducci C, Sznitman R, Kwong RY, Gräni C. Multiparametric cardiovascular magnetic resonance approach in diagnosing, monitoring, and prognostication of myocarditis. *JACC Cardiovascular Imaging*. (2022) 15(7):1325–38. doi: 10.1016/j.jcmg.2021.11.017
- Buckberg G, Hoffman JL, Mahajan A, Saleh S, Coghlan C. Cardiac mechanics revisited: the relationship of cardiac architecture to ventricular function. *Circulation*. (2008) 118(24):2571–87. doi: 10.1161/circulationaha.107.754424
- Götte MJW, Germans T, Rüssel IK, Zwaneburg JJ, Marcus JT, van Rossum AC, et al. Myocardial strain and torsion quantified by cardiovascular magnetic resonance tissue tagging: studies in normal and impaired left ventricular function. *J Am Coll Cardiol*. (2006) 48(10):2002–11. doi: 10.1016/j.jacc.2006.07.048
- Lee JW, Jeong YJ, Lee G, Lee NK, Lee HW, Kim JY, et al. Predictive value of cardiac magnetic resonance imaging-derived myocardial strain for poor outcomes in patients with acute myocarditis. *Korean J Radiol*. (2017) 18(4):643–54. doi: 10.3348/kjr.2017.18.4.643
- Lee J, Choo KS, Jeong YJ, Lee G, Hwang M, Abraham MR, et al. Left atrial strain derived from cardiac magnetic resonance imaging can predict outcomes of patients with acute myocarditis. *Korean J Radiol*. (2023) 24(6):512–21. doi: 10.3348/kjr.2022.0898
- Willenheimer R, Rydberg E, Stagmo M, Gudmundsson P, Ericsson G, Erhardt L. Echocardiographic assessment of left atrioventricular plane displacement as a complement to left ventricular regional wall motion evaluation in the detection of myocardial dysfunction. *Int J Cardiovasc Imaging*. (2002) 18(3):181–6. doi: 10.1023/a:1014664825080
- Rydberg E, Gudmundsson P, Kennedy L, Erhardt L, Willenheimer R. Left atrioventricular plane displacement but not left ventricular ejection fraction is influenced by the degree of aortic stenosis. *Heart*. (2004) 90(10):1151–5. doi: 10.1136/hrt.2003.020628
- Romano S, Judd RM, Kim RJ, Kim HW, Klem I, Heitner JF, et al. Left ventricular long-axis function assessed with cardiac cine mr imaging is an independent predictor of all-cause mortality in patients with reduced ejection fraction: a multicenter study. *Radiology*. (2018) 286(2):452–60. doi: 10.1148/radiol.2017170529
- Rangarajan V, Chacko SJ, Romano S, Jue J, Jariwala N, Chung J, et al. Left ventricular long axis function assessed during cine-cardiovascular magnetic resonance is an independent predictor of adverse cardiac events. *J Cardiovasc Magn Reson*. (2016) 18(1):35. doi: 10.1186/s12968-016-0257-y
- Spotnitz HM. Macro design, structure, and mechanics of the left ventricle. *J Thorac Cardiovasc Surg*. (2000) 119(5):1053–77. doi: 10.1016/s0022-5223(00)70106-1
- Geyer H, Caracciolo G, Abe H, Wilansky S, Carerj S, Gentile F, et al. Assessment of myocardial mechanics using speckle tracking echocardiography: fundamentals and clinical applications. *J Am Soc Echocardiogr*. (2010) 23(4):351–69, quiz 453–5. doi: 10.1016/j.echo.2010.02.015
- Luetkens JA, Schlesinger-Irsch U, Kuetting DL, Dabir D, Homs R, Doerner J, et al. Feature-Tracking myocardial strain analysis in acute myocarditis: diagnostic value and association with myocardial oedema. *Eur Radiol*. (2017) 27(11):4661–71. doi: 10.1007/s00330-017-4854-4
- Luetkens JA, Homs R, Sprinkart AM, Doerner J, Dabir D, Kuetting DL, et al. Incremental value of quantitative cmr including parametric mapping for the diagnosis of acute myocarditis. *Eur Heart J Cardiovasc Imaging*. (2016) 17(2):154–61. doi: 10.1093/ehjci/jev246
- Chen X, Hu H, Pan J, Shu J, Hu Y, Yu R. Performance of cardiovascular magnetic resonance strain in patients with acute myocarditis. *Cardiovasc Diagn Ther*. (2020) 10(4):725–37. doi: 10.21037/cdt-20-221
- Riordan MM, Kovács SJ. Relationship of pulmonary vein flow to left ventricular short-axis epicardial displacement in diastole: model-based prediction with *in vivo* validation. *Am J Physiol Heart Circ Physiol*. (2006) 291(3):H1210–5. doi: 10.1152/ajpheart.01339.2005
- Keren G, Sonnenblick EH, LeJemtel TH. Mitral annulus motion. Relation to pulmonary venous and transmitral flows in normal subjects and in patients with dilated cardiomyopathy. *Circulation*. (1988) 78(3):621–9. doi: 10.1161/01.cir.78.3.621
- Wang K, Ho SY, Gibson DG, Anderson RH. Architecture of atrial musculature in humans. *Br Heart J*. (1995) 73(6):559–65. doi: 10.1136/hrt.73.6.559
- Torrent-Guas F, Kocica MJ, Corno AF, Komeda M, Carreras-Costa F, Flotats A, et al. Towards new understanding of the heart structure and function. *Eur J Cardiothorac Surg*. (2005) 27(2):191–201. doi: 10.1016/j.ejcts.2004.11.026
- Henein MY, Gibson DG. Normal long axis function. *Heart*. (1999) 81(2):111–3. doi: 10.1136/hrt.81.2.111
- Carlsson M, Ugander M, Heiberg E, Arheden H. The quantitative relationship between longitudinal and radial function in left, right, and total heart pumping in humans. *Am J Physiol Heart Circ Physiol*. (2007) 293(1):H636–44. doi: 10.1152/ajpheart.01376.2006
- Zahid W, Johnson J, Westholm C, Eek CH, Haugaa KH, Smedsrud MK, et al. Mitral annular displacement by Doppler tissue imaging may identify coronary occlusion and predict mortality in patients with non-st-elevation myocardial infarction. *J Am Soc Echocardiogr*. (2013) 26(8):875–84. doi: 10.1016/j.echo.2013.05.011
- Brand B, Rydberg E, Ericsson G, Gudmundsson P, Willenheimer R. Prognostication and risk stratification by assessment of left atrioventricular plane displacement in patients with myocardial infarction. *Int J Cardiol*. (2002) 83(1):35–41. doi: 10.1016/s0167-5273(02)00007-4
- Sutherland GR, Di Salvo G, Claus P, D'Hooge J, Bijnens B. Strain and strain rate imaging: a new clinical approach to quantifying regional myocardial function. *J Am Soc Echocardiogr*. (2004) 17(7):788–802. doi: 10.1016/j.echo.2004.03.027
- Riffel JH, Andre F, Maertens M, Rost F, Keller MG, Giusca S, et al. Fast assessment of long axis strain with standard cardiovascular magnetic resonance: a validation study of a novel parameter with reference values. *J Cardiovasc Magn Reson*. (2015) 17(1):69. doi: 10.1186/s12968-015-0171-8
- Mayr A, Pamminger M, Reindl M, Greulich S, Reinstadler SJ, Tiller C, et al. Mitral annular plane systolic excursion by cardiac mr is an easy tool for optimized prognosis assessment in st-elevation myocardial infarction. *Eur Radiol*. (2020) 30(1):620–9. doi: 10.1007/s00330-019-06393-4
- Aquaro GD, Negri F, De Luca A, Todiere G, Bianco F, Barison A, et al. Role of right ventricular involvement in acute myocarditis, assessed by cardiac magnetic resonance. *Int J Cardiol*. (2018) 271:359–65. doi: 10.1016/j.ijcard.2018.04.087
- Bernhard B, Tanner G, Garachemani D, Schnyder A, Fischer K, Huber AT, et al. Predictive value of cardiac magnetic resonance right ventricular longitudinal strain in patients with suspected myocarditis. *J Cardiovasc Magn Reson*. (2023) 25(1):49. doi: 10.1186/s12968-023-00957-6
- Scatteia A, Pascale CE, Gallo P, Pezzullo S, America R, Cappelletti AM, et al. Abnormal papillary muscle signal on cine mri as a typical feature of mitral valve prolapse. *Sci Rep*. (2020) 10(1):9166. doi: 10.1038/s41598-020-65983-1
- Aquaro GD, De Gori C, Grilli G, Licordari R, Barison A, Todiere G, et al. Dark papillary muscles sign: a novel prognostic marker for cardiac magnetic resonance. *Eur Radiol*. (2023) 33(7):4621–36. doi: 10.1007/s00330-023-09400-x
- Deux JF, Maatouk M, Lim P, Vignaud A, Mayer J, Gueret P, et al. Acute myocarditis: diagnostic value of contrast-enhanced cine steady-state free precession mri sequences. *AJR Am J Roentgenol*. (2011) 197(5):1081–7. doi: 10.2214/ajr.10.6031